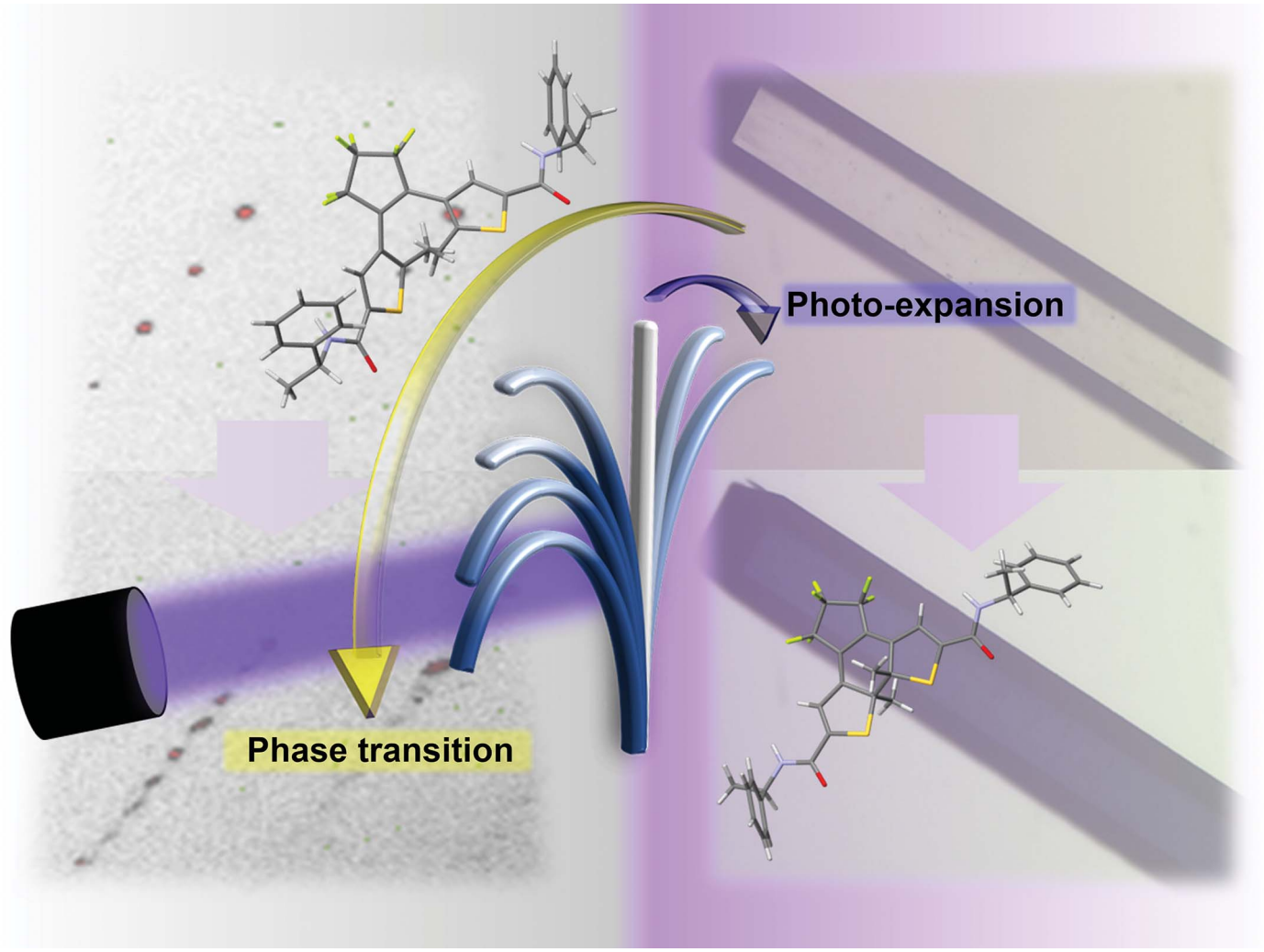

Showcasing research from Professor Uchida's laboratory, Department of Materials Chemistry, Ryukoku University, Otsu, Shiga, Japan.

Photoinduced swing of a diarylethene thin broad sword shaped crystal: a study on the detailed mechanism

Herein, a swinging motion of photochromic thin broad sword shaped crystals upon continuous irradiation with UV light was reported. The first slight bending away from the light source is due to photocyclization-induced surface expansion, and the second dramatic bending toward UV incidence is due to single-crystal-to-single crystal phase transition from the original phase I to phase II_{UV}. Upon visible light irradiation, the crystal returned to phase I. A similar phase transition with a similar volume decrease occurred by lowering the temperature.

As featured in:

See Kingo Uchida *et al.*, *Chem. Sci.*, 2020, **11**, 12307.

ROYAL SOCIETY OF CHEMISTRY

rsc.li/chemical-science

Registered charity number: 207890

Chemical Science

ROYAL SOCIETY OF CHEMISTRY

EDGE ARTICLE

View Article Online
View Journal | View Issue

Cite this: *Chem. Sci.*, 2020, **11**, 12307

All publication charges for this article have been paid for by the Royal Society of Chemistry

Photoinduced swing of a diarylethene thin broad sword shaped crystal: a study on the detailed mechanism†

Ayako Fujimoto,[a] Noriko Fujinaga,[a] Ryo Nishimura,[a] Eri Hatano,[a] Luna Kono,[a] Akira Nagai,[a] Akiko Sekine,[b] Yohei Hattori,[a] Yuko Kojima,[c] Nobuhiro Yasuda,[d] Masakazu Morimoto,[e] Satoshi Yokojima,[f] Shinichiro Nakamura,[g] Ben L. Feringa[h] and Kingo Uchida*[a]

We report a swinging motion of photochromic thin broad sword shaped crystals upon continuous irradiation with UV light. By contrast in thick crystals, photosalient phenomena were observed. The bending and swinging mechanisms are in fact due to molecular size changes as well as phase transitions. The first slight bending away from the light source is due to photocyclization-induced surface expansion, and the second dramatic bending toward UV incidence is due to single-crystal-to-single-crystal (SCSC) phase transition from the original phase I to phase II_{UV}. Upon visible light irradiation, the crystal returned to phase I. A similar SCSC phase transition with a similar volume decrease occurred by lowering the temperature (phase III_{temp}). For both photoinduced and thermal SCSC phase transitions, the symmetry of the unit cell is lowered; in phase II_{UV} the twisting angle of disordered phenyl groups is different between two adjacent molecules, while in phase III_{temp}, the population of the phenyl rotamer is different between adjacent molecules. In the case of phase II_{UV}, we found thickness dependent photosalient phenomena. The thin broad sword shaped crystals with a 3 μm thickness showed no photosalient phenomena, whereas photoinduced SCSC phase transition occurred. In contrast, large crystals of several tens of μm thickness showed photosalient phenomena on the irradiated surface where SCSC phase transition occurred. The results indicated that the accumulated strain, between isomerized and non-isomerized layers, gave rise to the photosalient phenomenon.

Received 29th September 2020
Accepted 13th October 2020

DOI: 10.1039/d0sc05388k

rsc.li/chemical-science

Introduction

Photochromic molecules that interconvert between two isomers, whose absorption bands are different from each other, have been studied for application in memories, switches and supramolecular systems.[1–5] Particularly, diarylethenes have been well studied for use in many applications,[6] followed by an intensive study in crystalline states.[7–15] Initially, Irie and co-workers reported the photo-induced bending and shape changes of the crystals of diarylethene derivatives.[7] They explained that the bending of the single crystal was attributed to the volume change of each molecule between open- and closed-ring isomers during photoisomerization.[9,10]

Reversible bending was observed not only for diarylethene derivatives but also for azobenzenes,[16] anthracene,[17] furylfulgides,[18] and salicylideneanilines[19] in their crystalline states, as well as liquid crystalline polymer films.[20–22] Particularly the photo-induced crystal movements of diarylethene derivatives are well studied among photochromic crystalline systems because of the thermal stability of the closed-ring isomer, for which the X-ray analysis of the photo-irradiated intermediate in the crystal was carried out. For example, photoinduced helical

[a]*Department of Materials Chemistry, Faculty of Science and Technology, Ryukoku University, Seta, Otsu, Shiga 520-2194, Japan. E-mail: uchida@rins.ryukoku.ac.jp; Fax: +81-77-543-7483; Tel: +81-77-543-7462*

[b]*Department of Chemistry, School of Science, Tokyo Institute of Technology, Ookayama 2-12-1, Meguro-ku, Tokyo 152-8551, Japan*

[c]*Materials Characterization Laboratory, Mitsubishi Chemical Corporation 1000, Kamoshida-cho, Aoba-ku, Yokohama 227-8502, Japan*

[d]*Japan Synchrotron Radiation Research Institute, 1-1-1 Kouto, Sayo-cho, Sayo-gun, Hyogo 679-5198, Japan*

[e]*Department of Chemistry and Research Center for Smart Molecules, Rikkyo University, Nishi-Ikebukuro 3-34-1, Toshima-ku, Tokyo 171-8501, Japan*

[f]*Tokyo University of Pharmacy and Life Science, Horino-uchi 1432-1, Hachioji, Tokyo 192-0392, Japan*

[g]*Nakamura Laboratory, RIKEN Cluster for Science, Technology and Innovation Hub, 2-1 Hirosawa, Wako, Saitama 351-0198, Japan*

[h]*Stratingh Institute for Chemistry, University of Groningen, Nijenborgh 4, 9747 AG Groningen, The Netherlands. E-mail: b.l.feringa@rug.nl; Fax: +31-50-363-4296*

† Electronic supplementary information (ESI) available. CCDC 1938354–1938363, 1938366, 1961657, and 1965755–1965757. For ESI and crystallographic data in CIF or other electronic format see DOI: 10.1039/d0sc05388k

twisting of the crystals[23] and photoinduced fragmentation of the crystals were reported.[24–27] Particularly photoinduced fragmentation and jumping of crystals were named the "photosalient effect" by Naumov.[24] Very recently complex behaviour in bending phenomena including twisting upon UV light irradiation was reported. It was based on the combination of a photochromic reaction and a reversible single-crystal-to-single-crystal (SCSC) phase transition.[28] Also, such photoinduced phenomena accompanied by phase transition of a salicylideneaniline derivative were reported.[29]

After the publication of our first paper concerning the bending phenomena of diarylethene crystals,[30] we observed the swinging motions under constant irradiation with UV light on the single crystals of a diarylethene derivative **1oRR** (Fig. 1a) with the thin broad sword shaped one prepared by sublimation. It underwent a dramatic concave bending toward the UV incidence followed by the reported backward bending under UV irradiation. The movements are summarized in Fig. 1b and ESI Movies 1 and 2.† Obviously the first backward swing motion is understood by photo-induced surface expansion. By contrast, the second is unexpected. We examined the cause of this drastic concave bending by preparing samples with different irradiation doses (*in situ* X-ray analysis), and observed a sudden change of diffraction spot numbers. This phase transition was studied in comparison with temperature-induced thermal phase transition. Finally, we reported the photosalient phenomena, since these phenomena are caused by phase transition depending on the thickness of the samples.

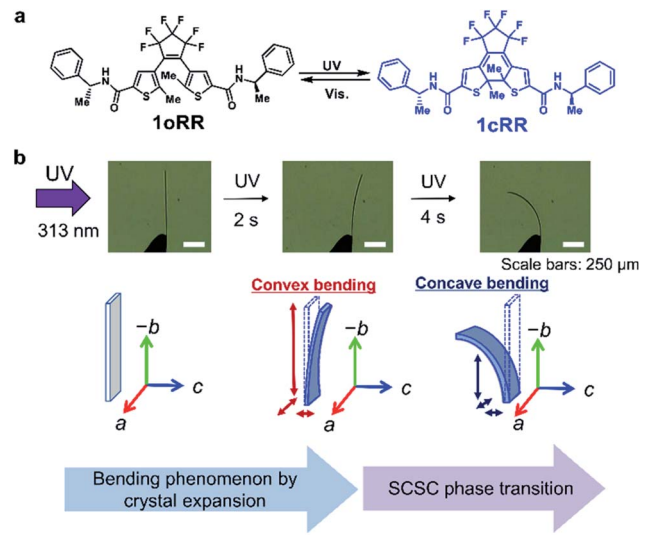

Fig. 1 (a) Molecular structures of **1oRR** and **1cRR**. (b) Bending behaviour of the thin broad sword shaped crystal upon UV light (313 nm) irradiation. Dimensions of the crystal were about 650 μm in length, 70 μm in width and 3 μm in thickness.

Results and discussion

Photoinduced swing of the 1oRR crystal

Upon UV irradiation of the thin crystal from the left side, the crystal bent slowly into a convex configuration, and then bent quickly into a concave configuration to the incidence of the light

Table 1 Photoinduced changes of the unit cell of the block **1oRR** crystal at 173 K[a]

	1oRR (initial)	**1oRR**-UV (after 313 nm light irradiation for 8 min)	**1oRR**-UV (after 313 nm light irradiation for 9 min)	**1oRR**-Vis. (after white LED light irradiation for 3 min)
T/K	173 (2)	173 (2)	173 (2)	173 (2)
Crystal system	Monoclinic	Monoclinic	Monoclinic	Monoclinic
Space group	$P2_1$	$P2_1$	$P2_1$	$P2_1$
a/Å	12.3769 (5)	12.457 (3) + 0.65%	12.131 (11) − 2.0%	12.851 (7) + 3.8%
b/Å	14.6220 (6)	14.737 (3) + 0.79%	14.308 (12) − 2.1%	14.275 (7) − 2.4%
c/Å	19.3798 (8)	19.461 (4) + 0.41%	36.28 (3) ($c'/2$ = 18.96–2.2%)[b]	19.163 (10) − 1.1%
α/°	90	90	90	90
β/°	106.751 (7)	107.079 (8) + 0.31%	91.678 (7) (β' = 106.97 + 0.21%)[c]	105.447 (7) − 1.2%
γ/°	90	90	90	90
V/Å^3	3358.4 (3)	3415.1 (13)	6294 (9)	3388 (3)
Volume for a molecule (Å^3)	839.6	853.8 + 1.6%	786.8–6.3%	847 + 0.88%
Z	4	4	8	4
R_1 ($I > 2\sigma(I)$)	0.0516	0.0597	0.0777	—
wR_2 ($I > 2\sigma(I)$)	0.1397	0.1591	0.2186	—
R_1 (all data)	0.0561	0.0798	0.1721	—
wR_2 (all data)	0.1447	0.1726	0.2743	—
CCDC	1938355	1938356	1938357	—

[a] The ratios of the unit cell change due to photoirradiation in comparison to initial structure **1oRR** are shown by percentage. [b] In order to compare the cell size before and after the phase transition, the half-length of the diagonal length between the *c* and *a* axes (c' axis) was compared. [c] The β′-angle is obtained as an angle formed by the *a*-axis and the diagonal line of the *a*- and *c*-axes. The angle was compared with the *β*-angle before phase transition. The details are described in Fig. S3.

(Fig. 1b and ESI Movies 1 and 2†). Upon irradiation of the resulting bent crystal from the same side using a 532 nm green diode laser, the crystal dramatically reverted to the convex-bent state, and gradually reverted to its initial straight position.

To clarify the details of the mechanism in this complicated bending phenomenon, we conducted XRD of the single crystal using synchrotron radiation (SPring-8).[31] Block crystals whose crystalline structure is the same as that of thin broad sword shaped crystals of **1oRR** were prepared by recrystallization from MeOH to monitor the structural changes upon UV irradiation (Tables 1 and S1, and Fig. S1†). Upon UV irradiation of the block crystal for 8 min, all the axes expanded about 0.3 to 0.8%. At this stage, closed-ring isomer **1cRR** generated by UV light irradiation was present at about 8% in the single crystal. After irradiation for an additional 1 minute, the number of diffraction spots suddenly increased approximately twice (Fig. 2 and S2†). Then, upon visible light irradiation, the number of diffraction spots returned to the initial value. This phenomenon is attributed to a photoinduced single-crystal-to-single-crystal (SCSC) phase transition. Herein, there are two possibilities for inducing phase transition.

(i) The photogenerated closed-ring isomer has a rigid six-membered-ring in its molecular structure,[32] and its original unit cell is different from the open-ring isomer, and therefore the photogenerated closed-ring isomers themselves induce a strain to the surrounding unit cells of **1oRR**, which works as a kind of pressure to induce the phase transition.[28,29]

(ii) During the first bending by expansion of the photo-irradiated side, the opposite side of the crystal suffers a compression to induce phase transition. However, the SCSC phase transition was also observed for rod-shaped crystals without bending. Therefore, the SCSC transition is attributed to the former mechanism of (i).

Analysis of the diffraction patterns showed that the c axis length expanded from 19.461 (4) to 36.28 (3) Å, the β angle contracted from 107.079 (8) to 91.678 (7)° and the number of the molecules in the unit cell increased from 4 to 8 after the SCSC phase transition. The transition induced the dramatic concave bending as shown in Fig. 1b.

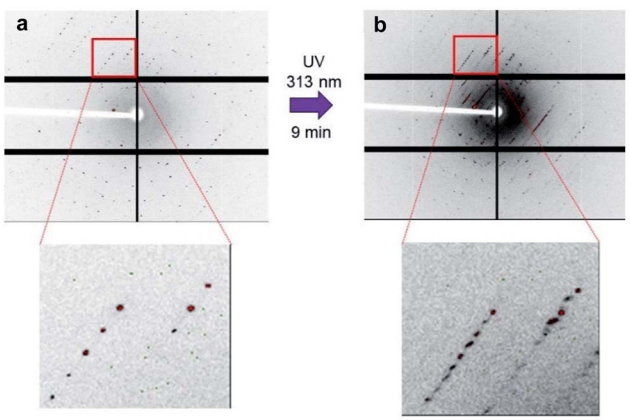

Fig. 2 Diffraction patterns (a) before and (b) after UV light (313 nm) irradiation for 9 min.

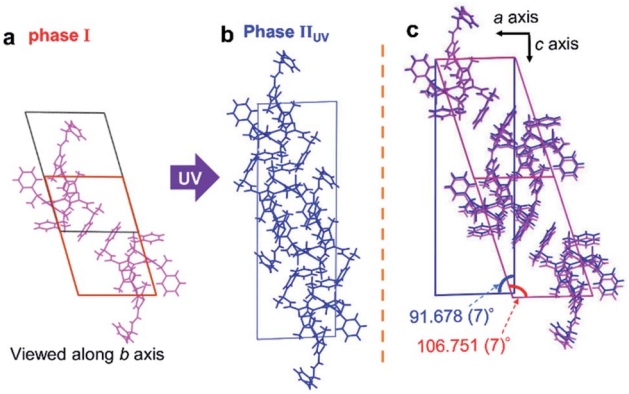

Fig. 3 Crystal structures viewed along the b axis (a) before and (b) after photoinduced SCSC phase transition and (c) overlapping of them.

Crystal phases before and after photoinduced SCSC phase transition are named phases I and II_{UV}, respectively. Viewing the crystal structure along the b axis, the shape of the unit cell of phase I is a parallelogram (red line in Fig. 3a), while that of phase II_{UV} is nearly a rectangle (blue line in Fig. 3b). Comparing β angles, the angles before and after photoinduced SCSC phase transition were 106.751 (7) and 91.678 (7)°, respectively. Comparing the overlapping diagram of the unit cells of phases I and II_{UV} (Fig. 3c), the overall unit cell contracted from phase I to phase II_{UV} as explained below. Although both crystal systems are monoclinic, the reduced cell of phase II_{UV} is different from the double of phase I; the β angle of phase II_{UV} is 91.678 (7)° which is near 90° relative to the β angle of phase I. Therefore, the c axis and the β angle before and after the phase transition cannot be directly compared. We took a new c' axis and β' angle for a new unit cell of phase II_{UV} as shown in Fig. S3.† Thus, we could discuss the change of $c'/2$ and β' which correspond to c and β in phase I. In the new unit cell of phase II_{UV}, all axes contracted about 2% and the volume for one molecule decreased about 6.3% compared to that in phase I (Table 1). This shrinkage corresponded to the dramatic concave bending of thin crystals in Fig. 1b. By X-ray single crystal structure analysis of phase II_{UV}, it was found that closed-ring isomer **1cRR** generated by UV light irradiation was present at about 10% in the blocky single crystal.

The mechanism of the photoinduced bending process can be interpreted by these changes of the unit cell. First, the crystal bended away from the light source because all axes expanded by the ring closure reaction near the surface. Then, as the ratio of the closed-ring isomer reached about 10% where most of the closed-ring isomers are concentrated near the surface, a phase transition occurred from phase I to phase II_{UV} at the surrounding unit cells of **1oRR**. Now it became clear that the second stage of bending toward the light source occurred, because the volume of the cell decreased rapidly by about 6.3%. Upon visible light irradiation for 3 min, the blue crystal turned to the initial colourless crystal, and along with it the number of diffraction spots decreased. Although we could not obtain the precise crystal structure after visible light irradiation, because the crystal became brittle by the salient phenomenon as we will

discuss later, we could determine a unit cell with a c axis of 12.851 (7) Å, β angle of 105.447 (7)°, and $Z = 4$ (Table 1). The photoinduced swing of the crystals upon alternate irradiation with UV and visible light was reversible. After repeating the photoinduced swing, the number of diffraction spots gradually decreased from the initial number, indicating the breaking of the crystal structure.

Comparing the crystal structures before and after photoinduced SCSC phase transition, the length of the c' axis of phase II_{UV} was almost doubled relative to the c axis of phase I. The number of molecules in a unit cell was also doubled from 4 to 8. In both crystals, the phenyl groups circled in Fig. 4a and b were disordered. Two phenyl group structures in red circles (shown in blue and magenta in Fig. 4d) were rotated about 80°. On the other hand, two phenyl group structures in a blue circle (shown in orange and pale blue in Fig. 4c) were slightly deviated and overlapping. In phase II_{UV}, the structure of the terminal phenyl group at the disordered moiety is different in two adjacent molecules, and thus the symmetry is lowered. Therefore, the cell could not be regarded as the same cell as phase I and, as a result, the c axis and the number of molecules in a unit cell doubled. The initial population ratios of the conformations of phenyl rings shown in dark blue and magenta coloured ones before UV irradiation at 173 K are 79 and 21%, respectively, from X-ray analysis (Fig. 4). After UV irradiation for 9 min, the ratio became 76 and 24%, respectively; besides the populations of disordered phenyl rings of orange and pale blue coloured ones are 57 and 43%, respectively (Fig. 4). Similar rotation of phenyl rings was also observed during the cooling process with shrinkage of the unit cell in the next section.

Thermal phase transition

Then we examined the possibility whether the SCSC phase transition can occur, not only with UV light but also by lowering the temperature. Cooling the crystals also induced shrinkage of the system. In fact, thermal SCSC phase transition occurred when the crystal cooled to 90 K (Fig. S4†). The low-temperature phase after thermal SCSC phase transition is observed as phase III_{temp} (Fig. 5b). The temperature of the thermal phase transition, which was determined by using differential scanning calorimetry (DSC), was 117 K (Fig. S5†). To compare crystal structures before and after the thermal SCSC phase transition, we measured the crystal structure at 173 and 90 K. When the crystal was cooled from 173 to 90 K at -5 K min^{-1}, the number of diffraction spots doubled from approximately 76 000 to 149 000 (Fig. S4†). When the temperature was increased to 173 K again at 10 K min^{-1}, the number of diffraction spots returned to the initial value. The observed thermal SCSC phase transition is quite similar to the photoinduced one. The cooling rate was critical for the thermal SCSC phase transition to occur. In fact, when the crystal was cooled below the phase transition temperature at a speed of -30 K min^{-1}, the phase transition never occurred. When the crystal was cooled at a speed of -5 K min^{-1}, the phase transition occurred. The transition was also monitored with the β angle of a unit cell (Fig. S6†).

As shown in Fig. 5b for phase III_{temp}, both disordered terminal phenyl rings circled in red and blue circles were rotated approximately 80° due to the strain accompanied by the SCSC phase transition. Although we showed here a similar SCSC transition by UV irradiation and temperature control, there is a difference in detail; one of the disordered terminal phenyl rings overlaps (Fig. 4d). Commonly, in the photoinduced phase transition, the increase of the ratio of **1cRR** in the surrounding

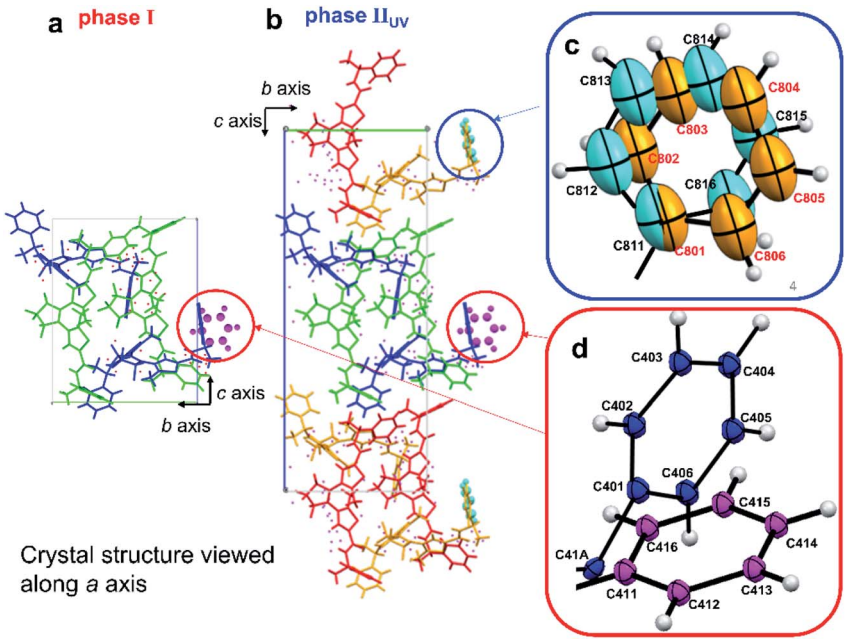

Fig. 4 Crystal structures from the (100) face of (a) phase I and (b) phase II_{UV}. (c) Enlarged view of disordered phenyl groups circled in blue. (d) Enlarged view of disordered phenyl groups circled in red.

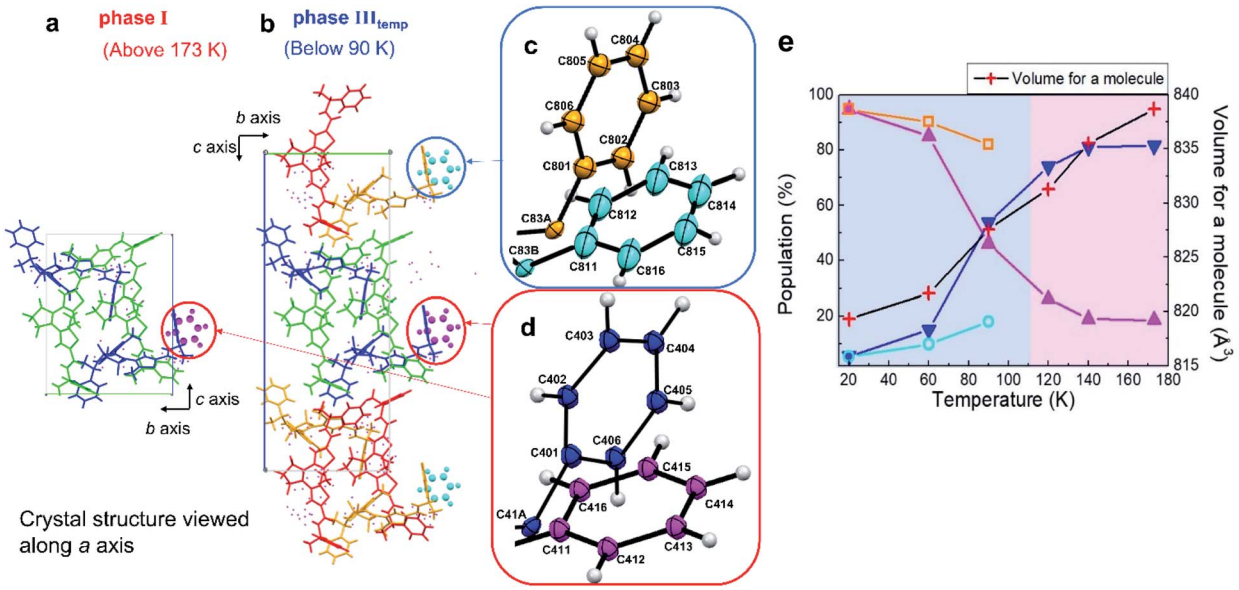

Fig. 5 Crystal structures (a) before and (b) after thermal SCSC phase transition viewed along the *a* axis. (c) Enlarged view showing phenyl groups of (b) circled in a blue line. (d) Enlarged view showing phenyl groups of (a) and (b) circled in a red line. (e) Temperature dependence of the population of the disordered phenyl groups. For increasing the temperature from 20 K to 173 K, the heating rate was 10 K min^{-1}. For the measurements of the crystal structure, the temperature was maintained for 20 min during the measurements. Dark blue and magenta lines correspond to the populations of dark blue and magenta coloured phenyl rings in (c), while pale blue and orange lines correspond to those of pale blue and orange coloured phenyl rings in (d). When the measurement temperature was below 110 K, the populations of the disordered phenyl groups between two adjacent molecules were different. Thus, symmetry is lowered, adjacent molecules were considered to be in different cells, the length of the *c* axis is doubled, and the number of molecules in the unit cell doubled from 4 to 8 (CCDC numbers: 1938358–1938363†).

1oRR lattice induced the strain which is the driving force of phase transition. Similarly, the contraction of the cell volume triggers the thermal phase transition.

To evaluate the percentage of the disordered phenyl rings, a crystal was analysed as a function of the temperature from 20 to 173 K with a heating speed at 10 K min^{-1} and its structures at each temperature were analysed (Fig. 5e). When the crystal of **1oRR** was cooled at 20 K, the percentages of phenyl rings shown in orange and pale blue (Fig. 5e) rotated approximately 80° were 95% and 5%, and those of disordered phenyl rings shown in blue and magenta were 5 and 95%, respectively. At 90 K, the population of the phenyl rings in blue and magenta gradually became closer, and finally reached the same population (around 50%).

On the other hand, the phenyl rings in orange and pale blue made up 80 and 20% of the population in the same range of the temperature, respectively. On increasing the temperature from 90 to 173 K above thermal SCSC phase transition, the percentage of the phenyl ring in blue and magenta became 80 and 20%, respectively. In addition, the SCSC phase transition showed hysteresis between the cooling and heating process. But, when the crystal was cooled and heated within the temperature range of phase I, the hysteresis was not observed (Fig. S7†). In the thermal phase transition case, the ratio of the terminal phenyl group at the disordered moiety is different between two adjacent molecules therefore the symmetry is lowered. Thus, the length of the *c* axis is doubled. To confirm whether the ratio of the disordered phenyl ring changes after a long time, we kept the crystal at 90 K for three hours. The ratio remained almost the same (Fig. S8†). The transformation of the single crystal of **1oRR** did not depend on the retention time, but only on the measurement temperature. The reversible and continuous phase transition was also observed by alternate cooling and heating. Therefore, we consider that the thermal phase transition of **1oRR** is a martensitic-like transformation.[33–35]

As the temperature decreased, the volume of a molecule gradually decreased due to thermal contraction. As shown in Table 2, comparing 20 K with 173 K, all axes contracted (see Fig. S3† for the comparison method), the volume for a molecule decreased by 19.4 Å^3 (−2.3%), the density increased by 0.031 g cm^{-3} (+2.4%), and the average distance of the intermolecular hydrogen bond decreased by 0.01 Å (−0.3%). To examine the

Table 2 Summary of the volume and density of **1oRR** depending on the measurement temperature

Temp. (K)	Volume of a unit cell (Å^3)	Volume of a molecule (Å^3)	Density (g cm^{-3})	Intermolecular hydrogen bonding distance (av.) (Å)
173	3354.8	839	1.312	2.864
20	6554.2	819–2.3%	1.343 + 2.4%	2.854 − 0.3%

contribution of the volume contraction by thermal SCSC phase transition, we performed the X-ray analysis of an orthorhombic polymorph crystal prepared by the vapour diffusion method of hexane vapor to THF solution with changing the temperature. The orthorhombic broad sword shaped crystal has a similar crystal structure to the monoclinic one but never gives rise to thermal SCSC phase transition. The contraction ratio of the orthorhombic crystal was almost the same as that of the monoclinic crystal of **1oRR**. We obtained the results which support these arguments (Table S2 and Fig. S9†). Therefore, it is considered that the volume contraction of **1oRR** was due to cooling to a low temperature.

For further consideration of the photoinduced bending of the crystal depending on the chirality of the molecular structure, we measured the single crystal of **1oSS** which has opposite chirality to **1oRR**. At 173 K, the crystal structure of **1oSS** was isomorphic to **1oRR**. When the crystal of **1oSS** was cooled to 80 K, thermal SCSC phase transition occurred similarly to that in **1oRR**.

Photosalient phenomena

The photoinduced scattering phenomenon of artificial crystals is called the photosalient effect.[36–38] During the analysis of bending phenomena of the thin crystals of **1oRR** upon UV irradiation at low temperatures at SPring-8, we often came across the photosalient phenomena. Herein the phenomena of **1oRR** crystals were described. Photogenerated stress due to the formation of isomers whose molecular size is different from that of the original one induces breaking of the crystals. In some cases, the peeling of the crystal surface proceeded due to the photogenerated size changes of the unit cells of crystals because the photoreaction mainly proceeds near the crystal surface. Upon UV light irradiation, the crystals of **1oRR** exhibited either bending or photosalient phenomena depending on the thickness of crystals (at that time conversions to the closed-ring isomer **1cRR** were less than 10%). We show these two results below. In the case of thin broad sword shaped crystals, bending occurs upon UV irradiation (Fig. 1b), however, cracking was not observed on the surface neither before nor after UV light irradiation (Fig. 6a and b). On the

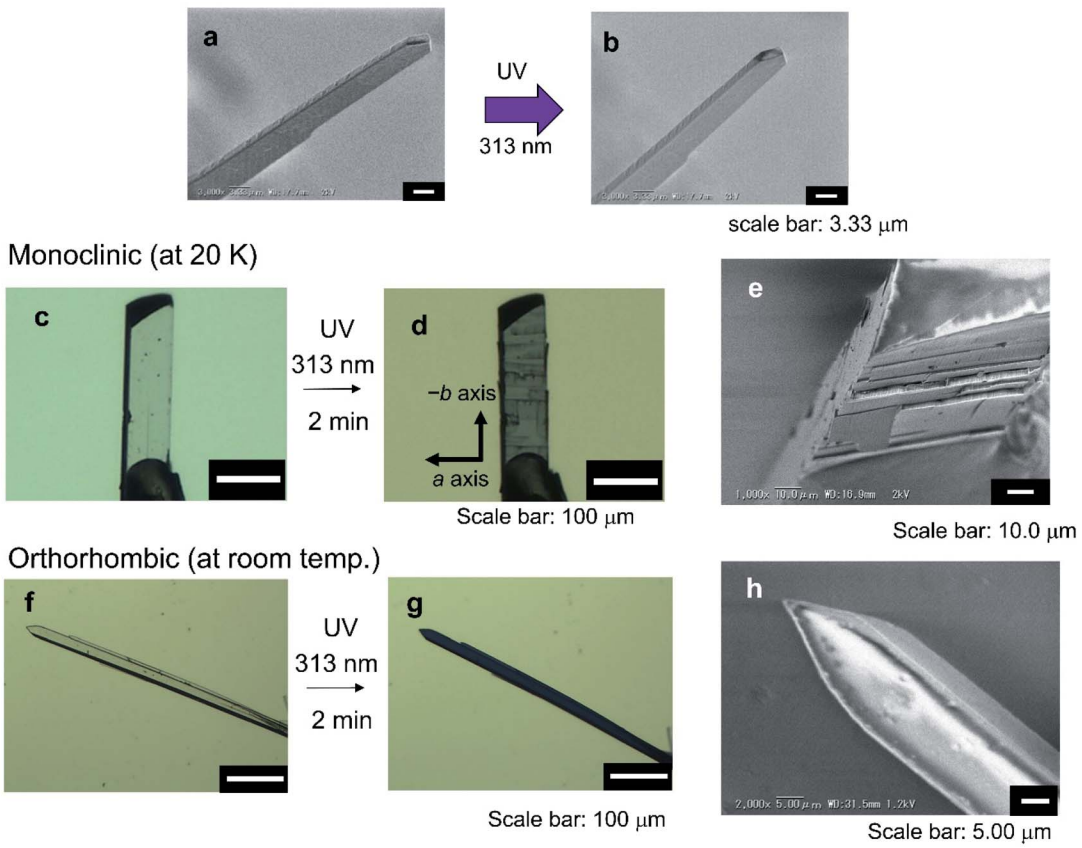

Fig. 6 Observation of bending and photosalient behaviour. Bending behaviour of the thin broad sword shaped crystal under UV light (313 nm) irradiation. SEM images of the surface (a) before and (b) after UV light irradiation, respectively. Upon UV irradiation of the surface of the thin broad sword shaped crystal, the crystal became coloured but not cracked, because the shrinkage was only 2%, which is much less compared with that of photoinduced SCSC phase transition. (c) Optical microscope image of the crystal prepared by recrystallization from MeOH. When this crystal was cooled from 150 K to 20 K at 5 K min^{-1}, no crack was observed on the crystal surface. (d) After UV light (313 nm) irradiation for 2 min keeping at 20 K, the crystal surface was peeled showing the photosalient phenomenon. (e) SEM image of the photosalient crystal of (d). The thickness of the ruptured area is about 1.0–2.5 μm. (f) Polymorph crystal of **1oRR** (orthorhombic) prepared by the vapor diffusion method of hexane vapor to THF solution. (g) Optical microscope image of the orthorhombic crystal after UV light irradiation for 2 min. (h) SEM image of (g). There were no cracks on the crystal surface. (a and b): scale bar = 3.33 μm. (c, d, f and g): scale bars = 100 μm. (e): scale bar = 10.0 μm. (h): scale bar = 5.00 μm.

other hand, when a single crystal of **1oRR** having a thickness of about several tens of μm was irradiated by UV light, the surface was peeled, and it showed the photosalient phenomenon (Fig. 6c–e). Within the 20–294 K temperature range, the photosalient phenomenon occurred (Fig. 6c–e and S10†). We noticed that the crystal peeled along a surface perpendicular to the *c* axis. The direction corresponded to the direction of the intermolecular hydrogen bond (NH–O, shown in Fig. S11†). Upon UV light irradiation, the crystal peeled along the *a* axis, because it was not able to withstand the distortion generated by formation of the closed-ring isomer. It is natural that surface peeling did not occur randomly, instead it occurs in parallel to the hydrogen bond, because the hydrogen bond remains as before the breaking.

Here let us now discuss the detailed mechanism of photosalient phenomena. Speaking first from the conclusion, most probably the phenomena are closely related to the photoinduced phase transition. The macroscopic experimental results are shown in Fig. 6. Our arguments are as follows.

First, we considered the reason why the crack appears on the surface of the block crystal of **1oRR**. Naturally, this is because the cyclization reaction occurred mainly on the surface of the crystal. Then, we tried to estimate the thickness of the photosalient depth on the surface of the crystal by observing the cross section of the crystal with SEM. The thickness from the surface was estimated to be 1.0–2.5 μm, which corresponds to the thickness of the thin broad sword shaped crystals. As a matter of fact, upon UV irradiation on such a thin broad sword shaped crystal, the strain due to the SCSC phase transition is mostly released by the bending of the crystal. On the other hand, in a block crystal, obviously the SCSC phase transition occurs only at the surface of the crystal. Therefore, the strain must be generated at the interface between the transition-occurred layer and unchanged deeper layer. This naturally induces cracking and peeling on the crystalline surface. In other words, the photoinduced phase transitions have a bending and swinging effect on the thin broad sword shaped crystal, whereas it gives the photosalient phenomena on a bulk crystal.

To verify this hypothesis, we carried out additional experiments by using the polymorph of **1oRR**. We prepared the crystals of **1oRR** by the vapor diffusion method of hexane vapor to THF solution (Fig. 6f–h and S9†), which is an orthorhombic broad shaped crystal without showing thermal SCSC phase transition as previously described. To our surprise, no salient phenomena were observed in this crystal in which the content of the photogenerated **1cRR** was almost 9%. The obtained orthorhombic crystal did not show SCSC phase transition by cooling to 20 K (Table S3†). The results show neither a temperature phase change nor photosalient phenomena on the orthorhombic crystal. (In fact, upon 313 nm light irradiation, the crystal shows only slight bending toward the incident light.) We can conclude that the photoinduced SCSC phase transition is critical for the photosalient phenomena to occur.

Conclusions

We succeeded in elucidating the bending mechanism in thin broad sword shaped crystals of **1oRR**. It is in fact due to the unit cell size changes. The smooth bending is due to the photochromic reactions, and dramatic bending is due to the SCSC phase transition. Upon 313 nm light irradiation, the block crystal of **1oRR** obtained by recrystallization from MeOH solution, which is isomorphic to the thin broad sword shaped crystal, had all its axes expanded by approximately 0.3 to 0.8%. Then photoinduced SCSC phase transition from phase I to phase II_{UV} occurred and suddenly the volume of a molecule decreased by 6.3%. It is revealed that when the photoinduced SCSC phase transition occurred, the thin broad sword shaped crystal bent concavely to the incidence of the light. Moreover, upon visible light irradiation, the crystal returned to phase I and SCSC phase transition occurred reversibly. Another SCSC phase transition occurred by changing the temperature (phase III_{temp}). The symmetry of the unit cell is lowered for both phases II_{UV} and III_{temp}, however, the mechanism of the lowering of symmetry differs. In phase III_{temp} the population of the phenyl rotamer is different in adjacent molecules in the crystal (Fig. 5) but in phase II_{UV} the twisting angle of disordered phenyl groups is different between two adjacent molecules (Fig. 4) and therefore the symmetry is lowered. In spite of the difference in the phenyl rotamer between phase II_{UV} and phase III_{temp}, there is the same tendency to increase the packing of the molecules; the phenyl rotamers of phase II_{UV} shown in orange and pale blue in Fig. 4 correspond to those of phase III_{temp} shown in orange in Fig. 5 at low temperatures such as 20 K. Additionally, the ratio of the phenyl rotamer of phase II_{UV} shown in magenta increased upon irradiation with UV light. The direction of the change of the ratio agrees with the increase of the ratio of the phenyl rotamer of phase III_{temp} shown in magenta by lowering the temperature. Even though the change of the ratio of the phenyl rotamer in phase II_{UV} is small, it is natural considering that the ratio of the closed-ring isomer is only 10%. Both SCSC phase transitions from I to II_{UV} and from I to III_{temp} were triggered by strain to shrink the unit cells of **1oRR**. Local free volumes around (*R*)-*N*-phenylethylamide groups calculated[39,40] from the crystal structures are decreased upon UV irradiation as well as cooling the crystal. The free volume of I (before UV irradiation) was 99.6 $Å^3$. Upon UV irradiation for 8 min, the volume reduced to 97.4 $Å^3$. After UV irradiation for 9 min, the volumes in Fig. 4c and d at the II_{UV} state are 77.4 and 83.9 $Å^3$, respectively. The remarkable reduction of the volume was observed after phase transition. The volume changes were also observed upon cooling the **1oRR** crystal. The volume reduced from 100.4 $Å^3$ (173 K) to 94.8 $Å^3$ (Fig. 5c) and 100.9 $Å^3$ (Fig. 5d) at 90 K, and 90.9 $Å^3$ (Fig. 5c) and 96.5 $Å^3$ (Fig. 5d) at 20 K. These data support the proposed mechanism.

We also succeeded in elucidating the relationship between the photosalient phenomenon and the crystal shape. The thin broad sword shaped crystals with a 3 μm thickness have never peeled because photoinduced SCSC phase transition occurred in the whole crystal. On the other hand, in large crystals with

a thickness of several tens of μm, we found that SCSC phase transition occurred only on the irradiated surface and gave rise to the photosalient phenomenon when the crystal was not able to withstand the distortion.

Experimental procedures

Methods

The diarylethene **1oRR** was synthesized according to previous literature.[30,31] Block crystals (monoclinic) of **1oRR** were prepared by recrystallization from MeOH solution. The broad sword shaped crystals (thickness *d*: ~20 μm) of **1oRR** (orthorhombic) were prepared by the vapor diffusion method of hexane vapor to THF solution. Thin broad sword shaped (monoclinic) crystals (thickness *d*: ~3 μm) of **1oRR** were obtained by sublimation on hotplates KPI Models HP-19U300P and HP-19U300 at 250 °C for 1 hour which is 20 °C below the melting point of **1oRR**. Thereafter, the crystals were cooled to room temperature. Molecular packing of these crystals was the same as the one in a previous paper,[41] and the distances of the reactive carbon atoms were less than 4.2 Å indicating that they are reactive in the crystalline state.[42] The 313 nm UV light-induced bending of the crystal and the subsequent recovery process upon 532 nm laser light irradiation were observed under an optical microscope.

UV hand lamp SPECTROLINE Model EB-280C/J ($\lambda = 313$ nm, 8 W) was used for UV irradiation of the thin and block crystals, and a white LED (SHODENSHA, AC100 ~240 V, max power consumption 17 VA, 5 W) was used as a visible light source. A Nikon OPTIPHOT2-POL equipped with a Shimadzu Moticam 2000 2.0 M Pixel USB2.0 was used for monitoring the crystal shape changes. SEM images were recorded on a Keyence VE-8800. DSC curves were recorded on a TA Instruments DSC 2920 by Japan thermal consulting Co., Ltd.

X-ray crystallographic analysis

X-ray crystallographic analysis for the thin and block crystals of **1oRR** was carried out at BL40XU and BL02B1 beamlines of SPring-8.

A beamline BL40XU: Si(111) channel cut monochromator was used and the wavelength and the size of the X-ray beam were 0.78229 Å and 75 × 75 μm (square), respectively. The diffraction data were collected by the oscillation method using an EIGER detector at 173 K. The data were corrected for absorption effects by a multi-scan method with ABSCOR.[43]

A beamline BL02B1: Si(311) double crystal monochromator was used and the wavelengths were 0.4146 Å, 0.4246 Å, and 0.42677 Å. The sizes of X-ray beams were 127 (H) × 120 (V) μm, 127 (H) × 176 (V) μm and 123 (H) × 128 (V) μm. The diffractometer was equipped with a PILATUS3 X CdTe 1M detector (DECTRIS Ltd, Baden, Switzerland) from 20 to 173 K.

The structures were determined by the direct method and refined by the full-matrix least-squares method using the SHELX-2014/7 program. The positions of all hydrogen atoms were calculated geometrically and refined by the riding model.

The conversions from **1oRR** to the closed-ring isomer **1cRR** in the crystals upon UV irradiation were determined by disorder analysis of crystallography. Upon UV irradiation, the superposition of **1oRR** and **1cRR** appeared. Then we determined the conversion by the disorder of sulphur atoms of thiophene rings of **1oRR** and **1cRR**.[44]

Conflicts of interest

There are no conflicts to declare.

Acknowledgements

We thank Dr Norio Urayama (Nihon Thermal Consulting Co., Ltd.) for DSC measurements of crystals at low temperatures. This work was supported by the Ministry of Education, Culture, Sports, Science and Technology, Japan (MEXT) as a Supported Program for the Strategic Research Foundation at Private Universities and by JSPS KAKENHI Grant Number JP26107012 in Scientific Research on Innovative Areas "Photosynergetics", the CREST program (JPMJCR17N2) of the Japan Science and Technology Agency, the Core-to-Core Program and JSPS KAKENHI Grant Number JP18J20078 in JSPS Research Fellow. B. L. F. acknowledges the Ministry of Education, Culture and Science of the Netherlands (Gravitation program no. 024.001.035). K. U.'s collaborative work with the University of Groningen, the Netherlands, was supported by the visiting scientists' program of Ryukoku University. The synchrotron radiation experiments were performed using the BL02B1, BL40B2 and BL40XU beamlines of SPring-8 with the approval of the Japan Synchrotron Radiation Research Institute (JASRI) (Proposal No. 2013A1219, 2014A1048, 2014B1213, 2015A1240, 2015B1215, 2016A1602, 2017A1084, 2017A1085, 2017A1120, 2017B1134, 2017B1135, 2017B1159, 2018A1104, 2018A1207, 2018A1208, 2018B1091, 2018B1092, 2018B1124, 2018B1674, 2019A1110, 2019A1403, 2019A1670, 2019A1741, 2019B1077, and 2020A1072).

Notes and references

1 *Photochromism*, ed. G. H. Brown, Wiley-Interscience, New York, 1971.
2 *Photochromism Molecules and Systems*, ed. H. Duerr and H. Bouas-Laurent, Elsevier, Amsterdam, 1990.
3 *Molecular Switches*, ed. B. L. Feringa, Wiley-VCH, Weinheim, 2001.
4 F. Lancia, A. Ryabchun and N. Katsonis, *Nat. Rev. Chem.*, 2019, **3**, 536–551.
5 J. J. D. de Jong, L. N. Lucas, R. M. Kellogg, J. H. van Esch and B. L. Feringa, *Science*, 2004, **304**, 278–281.
6 M. Irie, *Chem. Rev.*, 2000, **100**, 1685–1716.
7 M. Irie, T. Fukaminato, K. Matsuda and S. Kobatake, *Chem. Rev.*, 2014, **114**, 12174–12277.
8 M. Irie and K. Uchida, *Bull. Chem. Soc. Jpn.*, 1998, **73**, 985–996.
9 S. Kobatake, S. Takami, H. Muto, T. Ishikawa and M. Irie, *Nature*, 2007, **446**, 778–781.

10 M. Morimoto and M. Irie, *J. Am. Chem. Soc.*, 2010, **132**, 14172–14178.
11 F. Terao, M. Morimoto and M. Irie, *Angew. Chem., Int. Ed.*, 2012, **51**, 901–904.
12 S. Kobatake, H. Hasegawa and K. Miyamura, *Cryst. Growth Des.*, 2011, **11**, 1223–1229.
13 A. Spangenberg, R. Metivier, J. Gonzalez, K. Nakatani, P. Yu, M. Giraud, A. Leaustic, R. Guillot, T. Uwada and T. Asahi, *Adv. Mater.*, 2009, **21**, 309–313.
14 T. Yamaguchi, W. Taniguchi, T. Ozeki, S. Irie and M. Irie, *J. Photochem. Photobiol., A*, 2009, **207**, 282–287.
15 R. Nishimura, A. Fujimoto, N. Yasuda, M. Morimoto, T. Nagasaka, H. Sotome, S. Ito, H. Miyasaka, S. Yokojima, S. Nakamura, B. L. Feringa and K. Uchida, *Angew. Chem., Int. Ed.*, 2019, **58**, 13308–13312.
16 H. Koshima, N. Ojima and H. Uchimoto, *J. Am. Chem. Soc.*, 2009, **131**, 6890–6891.
17 L. Zhu, R. O. Al-Kaysi and C. J. Bardeen, *J. Am. Chem. Soc.*, 2011, **133**, 12569–12575.
18 H. Koshima, H. Nakaya, H. Uchimoto and N. Ojima, *Chem. Lett.*, 2012, **41**, 107–109.
19 H. Koshima, K. Takechi, H. Uchimoto, M. Shiro and D. Hashizume, *Chem. Commun.*, 2011, **47**, 11423–11425.
20 Y. Yu, M. Nakano and T. Ikeda, *Nature*, 2003, **425**, 145.
21 T. Ikeda, M. Nakano, Y. Yu, O. Tsutsumi and A. Kanazawa, *Adv. Mater.*, 2003, **15**, 201–205.
22 O. S. Bushuyev, M. Aizawa, A. Shishido and C. J. Barrett, *Macromol. Rapid Commun.*, 2017, 1700253.
23 D. Kitagawa, H. Nishi and S. Kobatake, *Angew. Chem., Int. Ed.*, 2013, **52**, 9320–9322.
24 P. Naumov, S. C. Sahoo, B. A. Zakharov and E. V. Boldyreva, *Angew. Chem., Int. Ed.*, 2013, **52**, 9990–9995.
25 D. Kitagawa, T. Okuyama, R. Tanaka and S. Kobatake, *Chem. Mater.*, 2016, **28**, 4889–4892.
26 E. Hatano, M. Morimoto, K. Hyodo, N. Yasuda, S. Yokojima, S. Nakamura and K. Uchida, *Chem.–Eur. J.*, 2016, **22**, 12680–12683.
27 H. Hatano, M. Morimoto, T. Imai, K. Hyodo, A. Fujimoto, R. Nishimura, A. Sekine, N. Yasuda, S. Yokojima, S. Nakamura and K. Uchida, *Angew. Chem., Int. Ed.*, 2017, **56**, 12576–12580.
28 D. Kitagawa, K. Kawasaki, R. Tanaka and S. Kobatake, *Chem. Mater.*, 2017, **29**, 7524–7532.
29 T. Taniguchi, H. Sato, Y. Hagiwara, T. Asahi and H. Koshima, *Commun. Chem.*, 2019, **2**, 19.
30 K. Uchida, S. Sukata, Y. Matsuzawa, M. Akazawa, J. J. D. de Jong, N. Katsonis, Y. Kojima, S. Nakamura, J. Areephong, A. Meetsma and B. L. Feringa, *Chem. Commun.*, 2008, **5**, 326–328.
31 Since it was difficult to measure thin broad sword shaped crystals with a thickness of only about 3 μm, the axis changes were observed using an isomorphic block crystal with a thickness of 40 to 70 μm, which was obtained by recrystallization from MeOH solution (Tables 1 and S1†). We confirmed that the crystal structures of thin broad sword shaped and block crystals are isomorphic by single crystal structure analysis. The results show that the unit cell was packed with two conformers crossing each other vertically (Fig. S1†), the crystal system was monoclinic, and the space group was $P2_1$.
32 S. Kobatake, M. Morimoto, Y. Asano, A. Murakami, S. Nakamura and M. Irie, *Chem. Lett.*, 2002, **31**, 1224.
33 L. Li, P. Commins, M. B. Al-Handawi, D. P. Karothu, J. M. Halabi, S. Schramm, J. Weston, R. Rezgui and P. Naumov, *Chem. Sci.*, 2019, **10**, 7327–7332.
34 M. K. Panda, T. Runcevski, S. C. Sahoo, A. A. Belik, N. K. Nath, R. E. Dinnebier and P. Naumov, *Nat. Commun.*, 2014, **5**, 4811.
35 M. T. Ruggiero, J. A. Zeitler and T. M. Korter, *Phys. Chem. Chem. Phys.*, 2017, **19**, 28502.
36 P. Naumov, S. C. Sahoo, B. A. Zakharov and E. V. Boldyreva, *Angew. Chem., Int. Ed.*, 2013, **52**, 9990–9995.
37 P. Naumov, S. Chizhik, M. K. Panda, N. K. Nath and E. Boldyreva, *Chem. Rev.*, 2015, **115**, 12440–12490.
38 Y. Nakagawa, M. Morimoto, N. Yasuda, K. Hyodo, S. Yokojima, S. Nakamura and K. Uchida, *Chem.–Eur. J.*, 2019, **25**, 7874–7880.
39 Y. Ohashi, K. Yanagi, T. Kurihara, Y. Sasada and Y. Ohgo, *J. Am. Chem. Soc.*, 1981, **103**, 5805–5812.
40 T. Nemoto, *Nihon Kessho Gakkaishi*, 2001, **43**, 275–277.
41 K. Uchida, M. Walko, J. J. D. de Jong, S. Sukata, S. Kobatake, A. Meetsma, J. van Esch and B. L. Feringa, *Org. Biomol. Chem.*, 2006, **4**, 1002–1006.
42 S. Kobatake, K. Uchida, E. Tsuchida and M. Irie, *Chem. Commun.*, 2002, 2804–2805.
43 T. Higashi, *ABSCOR*, Rigaku Corporation, Tokyo, Japan, 1995Soft.
44 T. Yamada, S. Kobatake, K. Muto and M. Irie, *J. Am. Chem. Soc.*, 2000, **122**, 1589–1592.